

doi: doi:10.1038/nclimate295

<http://www.nature.com/nclimate/journal/v6/n7/full/nclimate2957.html>

Evaluation of dynamic coastal response to sea-level rise modifies inundation likelihood

Erika Lentz^{*1}, E. Robert Thieler¹, Nathaniel G. Plant², Sawyer R. Stippa¹, Radley M. Horton³, Dean B. Gesch⁴

¹U.S. Geological Survey, Woods Hole MA

²U.S. Geological Survey, St. Petersburg, FL

³Center for Climate Systems Research, The Earth Institute, Columbia University, New York, NY and
NASA Goddard Institute for Space Studies, New York, NY

⁴U.S. Geological Survey, Sioux Falls, SD

*corresponding author, elentz@usgs.gov, 508-457-2238.

Sea-level rise (SLR) poses a range of threats to natural and built environments^{1,2}, making assessments of SLR-induced hazards essential for informed decision-making³. We develop a probabilistic model that evaluates the likelihood that an area will inundate (flood) or dynamically respond (adapt) to SLR. The broad-area applicability of the approach is demonstrated by producing 30x30 m resolution predictions for more than 38,000 km² of diverse coastal landscape in the northeastern United States (U.S.). Probabilistic SLR projections, coastal elevation, and vertical land movement are used to estimate likely future inundation levels. Then, conditioned on future inundation levels and the current land-cover type, we evaluate the likelihood of dynamic response vs. inundation. We find that nearly 70% of this coastal landscape has some capacity to respond dynamically to SLR, and we show that inundation models over-predict land likely to submerge. This approach is well-suited to guiding coastal resource management decisions that weigh future SLR impacts and uncertainty against ecological targets and economic constraints.

Future impacts from climate change, and particularly SLR⁴, are expected to be widespread in coastal areas². The northeastern U.S. coastal landscape encompasses a variety of environments that will respond differently to SLR according to their geomorphology, geologic setting, ecology, and level of development. Elevated water levels due to SLR will exacerbate coastal erosion and flooding^{1,5}, particularly along developed coasts that have substantial, fixed, low-elevation infrastructure and real estate². Coastal habitats provide breeding areas and migration corridors for many threatened or endangered species⁶. Thus, a significant management challenge for densely populated areas like the northeastern U.S. is to ensure the regional persistence of species, habitat, and ecosystems that are vulnerable to SLR. Knowing where available coastal habitat is likely to be resilient, transition to a new state, or require a buffer zone to accommodate landward translation is essential for developing management and resource allocation strategies that preserve the intrinsic values of the coastal system⁷.

The potential for both inundation and dynamic response exists for many coastal landscapes; however, SLR assessments typically focus on only one type of response. Inundation assessments flood

existing topography with a projected sea level³. Although inundation seems straightforward to evaluate in terms of vertical and horizontal extent, its rigorous application requires accounting for technical and data uncertainties⁸ as well as SLR uncertainties⁹. More importantly, this approach fails to include the dynamic response due to anthropogenic, ecologic¹⁰, or morphologic processes such as erosion and deposition—that drives coastal landscape evolution¹¹. Dynamic response assessments^{11, 12} tend to represent cross-shore sediment transport processes explicitly with highly parameterized models, and can be used to make probabilistic assessments¹³ via Monte Carlo methods and sensitivity analyses to communicate uncertainty¹⁴. Uncertainty affecting these approaches includes unknowns regarding rates and magnitudes of SLR, storminess, model parameter values, and the extrapolation from cross-shore profiles to spatially extensive domains. This uncertainty must be estimated via comparison to detailed observations.

As an alternative, we developed a data-driven coastal response (CR) model that considers both inundation and dynamic response using a range of SLR scenarios and datasets describing elevation and vertical land movement. We integrate these elements with land-cover information to assess CR likelihoods in the form of a dynamic probability, $DP = 1 - \text{Prob. (inundate)}$, using a Bayesian network (Figure 1). The modeling approach considers over 400 different combinations of input and output variables and incorporates their corresponding uncertainties, allowing distinctions between locations and environment types where current data and knowledge yield high-confidence predictions and where new information or better data are needed to resolve uncertain outcomes. The assessment covers coastal Maine through Virginia, and includes a region with a wide range of coastal development, infrastructure, and environments found globally; including uplands, barrier beaches, spits, islands, mainland beaches, cliffs, rocky headlands, estuaries, and wetlands. The study area is defined by the -10 and +10 m elevation contours and mapped as a 30 m grid.

To predict CR likelihoods (Figure 2), we first compute an adjusted land elevation with respect to projected sea levels:

$$AE = E - SL + VLM + \textit{uncertainties} \quad (1)$$

where AE represents the adjusted elevation with respect to a future sea level; E denotes the initial land elevation; SL is a projected sea level in the 2020s, 2030s, 2050s, or 2080s; and VLM gives the current rate of vertical land movement due to glacial isostatic adjustment, tectonics, and other non-climatic effects such as groundwater withdrawal and sediment compaction¹⁵. Sources of uncertainty in AE predictions include SLR projections, elevation data accuracy, vertical datum adjustments, and the interpolation of VLM rates from point data; these geospatially-explicit input uncertainties are propagated through the model to produce a probability mass function P(AE) for every grid cell (Figure 2c,d). Once generated, AEs are related through evaluation of their dynamic response potential with generalized land-cover information and used to produce a CR likelihood (Figures 1, 2).

Discretized AE predictions provide an estimated submergence level comparable to many existing inundation models^{3, 16} (Figure 2). However, our predictions include several notable improvements over existing approaches: 1) SLR projections are associated with time, provided as a series of probabilistic decadal estimates aligning with planning and management timeframes; 2) we include VLM, ensuring relative SLR change is captured; and 3) our probabilistic AE predictions include robust uncertainty assessments. Despite these differences, it is possible to compare these results with inundation models^{3, 16} as an initial test of consistency (Figure 2a). Because we are forecasting sea levels for which observations do not exist, this initial test provides context for interpreting the subsequent CR predictions.

CR predictions augment inundation predictions by showing where dynamic response due to ecologic or morphologic processes is likely under a range of SLR scenarios (Figures 1, 2b). DP is high in areas likely to preserve their current land-cover state or transition to another non-submerged state by adapting to SLR. Inundation occurs in areas unlikely to adapt in these ways. For example, an upland environment may persist with SLR and remain upland or transition to a marsh; a marsh may vertically accrete to maintain itself, migrate laterally, or fail to keep pace with SLR and become inundated^{10, 17}.

CR thresholds for specific land-cover types—based on a synthesis of published studies on SLR-induced change^{10, 17-19}—were used where available to define persistence and determine a DP (Figure 1b). Where such information was unavailable, we assigned DPs to the remaining categories, following existing approaches used to fill information gaps with expert knowledge^{20, 21}. The potential for lateral translation of some environment types (marshes, forests, and beaches) is not directly incorporated into our model; however, the co-occurrence of increasing DP and increasing elevation tends to capture this behavior (Figure 1b). Probability assignments and how they relate to SLR thresholds are presented in Supplementary Information²².

The DP assignments in this study (Figure 1b) show that knowledge of particular outcomes is strongly related to elevation, and better understood for some land cover types (e.g. beaches) than for others (e.g. developed and forest). Elevation is an important first-order determinant of the spatial distribution of land-cover type (e.g. salt marshes occur at low elevations; forests occur at higher elevations), and land-cover types in end-member elevation ranges are more likely to maintain their predicted response type through time, indicated by high (> 0.75) or low (< 0.4) DP values. For example, areas with AEs that exceed projected SLR are expected to remain dry and maintain their current land-cover type through dynamic response, whereas areas already submerged are anticipated to become even more inundated, regardless of land-cover type. At moderate AEs, a number of physical-process components not addressed by the model (e.g. beach sediment supply; marsh accretion rate; human landscape modification) and land-cover-specific AE thresholds make CR predictions highly uncertain (e.g. DP ~ 0.5 , Figure 1). Thus, developed areas close to sea level, or beach areas that have an AE of -1 m have similar uncertainties in CR. Our approach allows any of these probability estimates to be updated as knowledge of coastal responses improves.

Comparison of AE and CR predictions for two time periods demonstrates the impact of changing SL on uncertainties (Figure 3). Initially nearly 70% of the region has potential for dynamic response²² (Figure 3), suggesting that for the majority of the Northeastern U.S. an inundation approach does not

adequately describe the SLR response. A highly dynamic location, such as Prime Hook National Wildlife Refuge (Figure 3a), shows 70% of the area is predicted to be submerged in 2020 (i.e., $AE < 0$) although the CR shows only 2% of the area is likely to inundate ($DP < 0.5$). The difference comes from the predicted dynamic response of the marsh, and demonstrates the importance of including this information to depict more realistically SLR effects on the landscape. As expected, there is a trend toward increased submergence ($AE < 0$) and greater prediction uncertainty through time for both AE and CR. This behavior is largely attributable to the SLR projections and their associated uncertainties; 2080s sea-level projections are the highest and the most uncertain, which are in turn reflected in wider probability distributions for predicted outcomes (Figure 3b).

SLR projections and associated uncertainties have the greatest effects on land at moderate initial elevations (-1 to 0 m and 0 to 1 m). For each land-cover type, we can identify when our knowledge of the CR is most uncertain (i.e., $DP = 0.5$) and when we are likely to observe a transition from dynamic response to inundation, indicating a SLR threshold has been exceeded (Figure 4). Here we relate our numerical CR predictions to verbal equivalents following the Intergovernmental Panel on Climate Change Fifth Assessment Report²³. At elevations of -1 to 0 m, developed areas are *likely* (66-100% probability) to inundate before the 2020s (relative to the base period of 2010), and marshes and forests after the 2030s. In the 0 to 1 m range, inundation is *likely* for developed areas by the 2050s, and marshes and forests by the 2080s. At any time step, rocky areas are *likely* to inundate, whereas beaches are *likely* to *very likely* (90-100% probability) to respond dynamically. Subaqueous environments are *likely* to be dynamic at any elevation range and time as they are expected to maintain their initial land-cover state; however those found below MHW have a greater DP than inland water bodies above MHW (Figure 4), presumably because they are responding to changes in sediment transport and resuspension, waves, tides, and other factors.

Model predictions provide a broad view of the coastal response to SLR and other processes at resolutions commensurate with landscape-scale decision-support needs. The different scenarios depict

potential landscape changes that can be used to quantify uncertainties, define a planning horizon, or improve an understanding of risk tolerance¹⁴. This information can guide decisions regarding land use and management, and provides context needed for understanding tradeoffs that may be necessary to achieve management goals, such as future land acquisitions or identification of land area buffers for ecosystem migration. Furthermore, the approach presented here is sufficiently generic to apply at other coastal locations globally where environments are similar but data may be more limited in availability or resolution. Probabilistic outcomes can help prioritize where future research efforts are directed to improve forecast capability, and as knowledge improves—for example due to better understanding of ice sheet behavior²⁴, storminess²⁵, adaptation actions¹, or more detailed morphologic and ecologic process information²—the model and predictions can be updated.

Understanding which response—inundation or dynamic—best describes the future system state over broad coastal landscapes can inform appropriate selection of more detailed modeling approaches. In some locations, submergence may be the most pressing problem and properly applied inundation models can adequately depict future conditions. Where complex coastal processes affect the landscape, detailed morphological models¹¹⁻¹³ may be best suited to explore future scenarios. Our modeling framework demonstrates comprehensive consideration of both response types is possible through an approach that can be applied to a variety of coastal settings, over a given time frame, or amount of SLR.

REFERENCES

1. Horton, R. *et al.* in *Climate Change Impacts in the United States: The Third National Climate Assessment* (eds Melillo, J. M., Richmond, T.C., and Yohe, G. W.) 371-395 (U.S. Global Change Research Program, 2014).
2. Wong, P.P. *et al.* in *Climate Change 2013: The Physical Science Basis*. (eds Stocker, T.F. *et al.*) 361-409 (Cambridge Univ Press, 2014).
3. Strauss, B.H., Ziemiński, R., Weiss, J.L., and Overpeck, J.T. Tidally adjusted estimates of topographic vulnerability to sea level rise and flooding for the contiguous U.S. *Environ. Res. Lett* **7**, 014033 (2012).
4. Church, J. A., *et al.* in *Climate Change 2013: The Physical Science Basis* (eds Stocker, T.F. *et al.*) 1137-1216 (Cambridge Univ Press, 2014).
5. Sweet, W. V., and Park, J. From the extreme to the mean: Acceleration and tipping points of coastal inundation from sea level rise, *Earth's Future* **2**, 579–600 (2014).
6. Gieder, K.D., *et al.* A Bayesian network approach to predicting nest presence of the federally-threatened piping plover (*Charadrius melodus*) using barrier island features. *Ecol. Modell* **276**, 38-50 (2014).
7. Peterson, G.D., Cumming, G.S., and Carpenter, S.R. Scenario planning: a tool for conservation in an uncertain world. *Conserv. Biol.* **17**, 358-366 (2003).

8. Gesch, D.B. Analysis of lidar elevation data for improved identification and delineation of lands vulnerable to sea-level rise. *J. Coastal Res.* **SI 53**, 49–58 (2009).
9. Parris, A.P., *et al.* *Global Sea Level Rise Scenarios for the US National Climate Assessment* (NOAA Tech Memo OAR CPO-1, 2012).
10. Kirwan, M.L., *et al.* Limits on the adaptability of coastal marshes to rising sea-level. *Geophys. Res. Lett.* **37**, L23401 (2010).
11. Cowell, P.J., Roy, P.S., and Jones, R.A. Simulation of large-scale coastal change using a morphological behavior model. *Mar. Geol.* **126**, 45-61 (1995).
12. Ranasinghe, R., Callaghan, D., and Stive, M. Estimating coastal recession due to sea level rise: Beyond the Bruun Rule. *Climatic Change* **110**, 561-574 (2012).
13. Wainwright, D. J., *et al.* Moving from Deterministic towards Probabilistic Coastal Hazard and Risk Assessment: Development of a Modelling Framework and Application to Narrabeen Beach, New South Wales, Australia. *Coast. Eng.* **96**, 92-99 (2015).
14. National Research Council. *Science and Decisions: Advancing Risk Assessment* (The National Academies Press, 2009).
15. Kopp, R. E., *et al.* Probabilistic 21st and 22nd century sea-level projections at a global network of tide-gauge sites. *Earth's Future* **2**, 383-406 (2014).

16. Marcy, D., *et al.* in *Proceedings of the 2011 Solutions to Coastal Disasters Conference* (eds Wallendorf, L., Jones, C., Ewing, L., and Battalio, R.) 474-490 (American Society of Civil Engineers, 2011).
17. Cahoon, D.R., *et al.* in *Coastal Sensitivity to Sea-Level Rise: A Focus on the Mid-Atlantic Region. A report by the U.S. Climate Change Science Program and the Subcommittee on Global Change Research.* (lead author, Titus, J.G.) 57-72 (U.S. Environmental Protection Agency, 2009).
18. Clark, J. S. Coastal Forest Tree Populations in a Changing Environment, Southeastern Long Island, New York. *Ecol. Monogr.* **56**, 259-277 (1986).
19. Gutierrez, B.T., Williams, S.J., and Thieler, R.T. in *Coastal Sensitivity to Sea-Level Rise: A Focus on the Mid-Atlantic Region. A report by the U.S. Climate Change Science Program and the Subcommittee on Global Change Research.* (lead author, Titus, J.G.) 43-56 (U.S. Environmental Protection Agency, 2009).
20. Bamber, J. L., and Aspinall, W. P. An expert judgment assessment of future sea-level rise from the ice sheets. *Nature Clim. Change* **3**, 424-427 (2013).
21. Horton, B.P., Rahmstorf, S., Engelhart, S.E., and Kemp, A.C. Expert assessment of sea-level rise by AD2100 and AD 2300. *Quat. Sci. Rev.* **84**, 1-6 (2014).
22. Lentz, E.E. *et al.* *Evaluating the Coastal Landscape Response to Sea-Level Rise for the Northeastern U.S.: Approach and Methods* (U.S. Geological Survey Open-File Report 2014-1252, 2015).

23. Mastrandrea, M.D., *et al.* *Guidance Note for Lead Authors of the IPCC Fifth Assessment Report on Consistent Treatment of Uncertainties* (Intergovernmental Panel on Climate Change, 2010).
24. Alley, R. B. *et al.* Oceanic Forcing of Ice-Sheet Retreat: West Antarctica and More. *Annual Review of Earth and Planetary Sciences* **43**, 207-231 (2015).
25. Knutson, T.R., *et al.* Tropical cyclones and climate change. *Nature Geosci.* **3**, 157-163 (2010).

Please direct correspondence and requests for materials regarding this manuscript to:

Erika Lentz, U.S. Geological Survey, Woods Hole Coastal and Marine Science Center, 384 Woods Hole Rd. Woods Hole, MA, 02543, USA, email: elentz@usgs.gov

ACKNOWLEDGMENTS

This research was funded by the U.S. Geological Survey Coastal and Marine Geology Program, the Department of the Interior Northeast Climate Science Center, and the U.S. Army Corps of Engineers Institute for Water Resources under the Responses to Climate Change Program. We thank Ben Strauss at Climate Central's Surging Seas project for permission to use their base map in Figure 2, and Carolyn Ruppel and Meagan Gonnee for early reviews and discussion of this manuscript. Any use of trade, firm, or product names is for descriptive purposes only and does not imply endorsement by the U.S. Government.

AUTHOR CONTRIBUTIONS

ERT and NGP developed the concept; EEL, NGP, and ERT conceptualized and designed the model; NGP built the model; EEL and SRS performed the model runs; EEL assessed and analyzed the data; RMH

contributed the SLR projections; DBG contributed regional elevation data; EEL, ERT, and NGP co-wrote the paper with input from all co-authors.

COMPETING FINANCIAL INTERESTS

The authors declare no competing financial interests.

FIGURES

Figure 1. Schematic diagram showing a) the conceptual coastal response model where x indicates dependence on the geospatial location and t indicates dependence on time; and b) the coastal response (CR) assignments presented as dynamic probability (DP) based on adjusted elevation range and land cover type; inundation probability is $1 - DP$. For example, if adjusted elevation is in the range of 0 to 1, the probability that a marsh environment will respond dynamically is 0.65.

Figure 2. Comparison showing: a) Surging Seas inundation map under 1.5 m of SLR (used with permission: <http://ss2.climatecentral.org/#13/42.7573/-70.8059?show=satellite&level=4&pois=show>); b) predicted coastal response likelihoods for 2080s sea level scenario (comparable projected SL to a); c) most-probable 2080s adjusted elevation (AE, or inundation levels); and d) probabilities of the AE values in (c).

Figure 3. Regional map (a) showing the spatial extent of predictions (gray shading) and examples of adjusted elevation (AE) and coastal response (CR) predictions for the 2020s and 2080s at Prime Hook National Wildlife Refuge in Delaware. The modeled probability distributions (b) for sea level (SL), AE, and CR are shown for each time step at a single cell location (black arrow in lower right panel of (a) indicates location).

Figure 4. Plots showing shifting coastal response (CR) likelihoods for each land cover type through time conditioned on moderate initial (present day) elevations (E). Central column shows the total percent of the prediction area comprised by each land-cover type by each E range. Red shows probability of dynamic response and blue shows probability of inundation.

METHODS

Our model uses a Bayesian network (BN), which we exploit here for its ability to propagate uncertainty, perform inference and calculate conditional probabilities, and structure the integration of stochastic, deterministic, and expert relationships. BNs have been applied to a variety of coastal problems^{6, 26, 27}, and output results in a probabilistic form well-suited to address decision-support needs. The relationships between parameters in a BN are established through directed links (causal relationships, Figure 1) which represent conditional probabilities trained on observations, probabilistic or deterministic equations, or expert opinion. An advantage in using BNs is their robust consideration of uncertainty. Uncertainties in the relationships derived from the observational training and uncertainties in the input parameters are propagated through the BN to provide a predicted probability for each discrete outcome. The training 1) captured the co-occurrence of land cover and elevation inputs, 2) used explicit relationships and input uncertainties among parameters as defined by equation (1), and 3) assigned dynamic response probabilities (DP) to a conditional probability table (CPT) based on knowledge specific to each scenario of land-cover (LC) and adjusted elevation²² (AE) to generate a coastal response (CR) prediction.

Our BN stores conditional probabilities in order to make predictions using combinations of statistical inference and joint probability calculations. For AE we use

$$P(AE_i) = \sum_{E,SL,VLM,LC} P(AE_i|E, SL, VLM) P(E|LC) P(SL_j) P(VLM_j) P(LC_j), \quad (2A)$$

where we evaluate the i^{th} AE outcome from 5 discrete possibilities; the summation accounts for uncertainties in the input variables; the first term on the right is the probabilistic relationship for equation (1) conditioned on inputs from the j^{th} spatial location at a particular time; and the second term accounts for the relationship between LC and elevation which is updated using Bayes theorem²²

$$P(E_i|LC_j) = P(LC_j|E_i) \times P(E_i) / P(LC_j). \quad (2B)$$

The remaining (independent) terms in equation 2A are updated with input from data or model sources, and are, in general, uncertain. The only exception is LC, which is entered as if known with certainty for each grid cell, as uncertainty for this term is unquantified²². As noted in this paper, there is an inherent correlation between current elevation and LC; capturing this relationship through inference training (Bayes' rule), allows us to use LC information to update the prior elevation information (based on the values of the digital elevation model [DEM] over the entire domain) and constrain elevation uncertainties attributed to errors in the DEM. For CR, we have

$$P(CR_i) = \sum_{AE,LC} P(CR_i|LC, AE) P(AE|LC) P(LC_j), \quad (2C)$$

where $P(AE)$ is computed from 2A (and depends on SL, VLM, E, as well as LC) and $P(CR_i|LC, AE)$ are determined from published work or expert knowledge^{10, 17-19}. In our implementation, LC is exact as noted above and so the summation is only performed over the AE values—but using the BN allows for uncertainty in LC and we would apply this capability if the land-cover maps included uncertainty.

Regional SLR projections were generated using multiple sources including scenarios—Representative Concentration Pathways (RCPs)—in the 2014 Intergovernmental Panel on Climate Change (IPCC) Fifth Assessment Report (AR5)²⁸. A three-component approach²⁹ for the SLR projections included an ocean term (including thermal expansion and local ocean height); ice melt; and land water storage. The ocean term is taken from 24 Coupled Model Intercomparison Project 5 (CMIP5) models³⁰ (http://cmip-pcmdi.llnl.gov/cmip5/data_portal.html); while the first part is global, the second is computed on a $1^\circ \times 1^\circ$ grid and extracted at the nearest ocean grid cell to each grid point in our domain. Ice melt

was estimated for the Greenland Ice Sheet and the two Antarctic Ice Sheets²⁰, and the glaciers and ice caps^{31,32}. Land water storage was based on IPCC AR5 WG1⁴. Set percentiles (10th, 25th–75th, and 90th) were estimated for each of the three components of sea-level change. These projection ranges are representative of key uncertainties in sea-level rise components.

SLR projections at each time interval (2020s, 2030s, 2050s, or 2080s) were initialized with uniformly distributed prior probabilities and updated with the regional projection probabilities (Figure 3b). Vertical land movement rates were estimated from GPS data³³ and tide station records³⁴. The highest resolution elevation data available (either ~3 m or ~10 m horizontal resolution; +/- 43 cm or 1.25 m vertical) through the National Elevation Dataset (NED)³⁵ were vertically adjusted to the MHW datum; bathymetry data at coarser resolution (~30 m) from the Coastal Relief Model were used in areas of open water. To represent coastal landscape types, we generalized regional land cover data into six categories based on established differences in physical and biological processes that drive responses to SLR²².

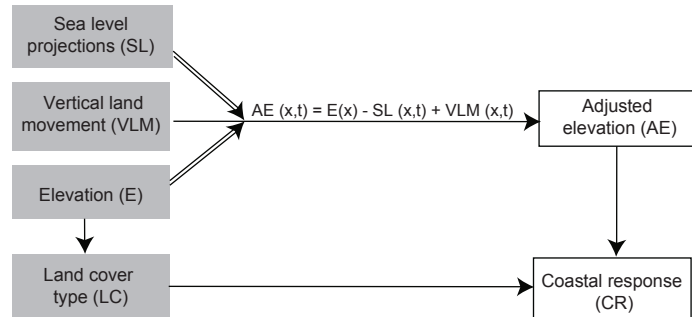
Results span the coastal zone from initial elevations of 10 m inland to -12 m offshore. A comprehensive discussion of methods and input datasets can be found in Supplementary Information²².

REFERENCES

26. Plant, N. G., and H. F. Stockdon, Probabilistic prediction of barrier-island response to hurricanes. *J. Geophys. Res.* **117**, F03015 (2012).
27. Gutierrez, B.T., Plant, N.G., and Thieler, E.R. A Bayesian network to predict the coastal vulnerability to sea-level rise: *J. Geophys. Res.* **116**, F02009 (2011).

28. Moss, R.H., *et al.* The next generation of scenarios for climate change research and assessment. *Nature* **463**, 747-756 (2010).
29. Horton, R., *et al.* New York City Panel on Climate Change 2015 Report Chapter 2: Sea Level Rise and Coastal Storms: *Ann. N. Y. Acad. Sci.* **1336**(1), 36-44 (2015).
30. Taylor, K. E., Stouffer, R. J., and Meehl, G. A. An Overview of CMIP5 and the Experiment Design. *Bull. Am. Meteorol. Soc.* **93**, 485-498 (2012).
31. Marzeion, B., Jarosch, A. H., and Hofer, M. Past and future sea-level change from the surface mass balance of glaciers. *The Cryosphere* **6**, 1295-1322 (2012).
32. Radić, V., *et al.* Regional and global projections of twenty-first century glacier mass changes in response to climate scenarios from global climate models. *Clim. Dyn.* **42**, 37-58 (2013).
33. Sella, G.F., *et al.* Observation of glacial isostatic adjustment in “stable” North America with GPS. *Geophys. Res. Lett.* **34**, L02306 (2007).
34. Zervas, C., Gill, S., and Sweet, W. *Estimating Vertical Land Motion from Long-Term Tide Gauge Records* (NOAA Technical Report NOS CO-OPS 065, 2013).
35. Gesch, D.B. in *Digital Elevation Model Technologies and Applications: The DEM User's Manual, 2nd Edition* (ed. Maune, D.) 99-118 (American Society for Photogrammetry and Remote Sensing, 2007).

a.



b.

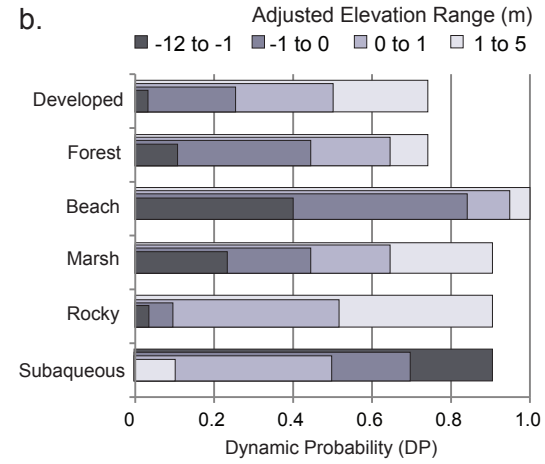


Figure 1. Schematic diagram showing a) the conceptual coastal response model where x indicates dependence on the geospatial location and t indicates dependence on time; and b) the coastal response (CR) assignments presented as dynamic probability (DP) based on adjusted elevation range and land cover type; inundation probability is $1 - DP$. For example, if adjusted elevation is in the range of 0 to 1, the probability that a marsh environment will respond dynamically is 0.65.

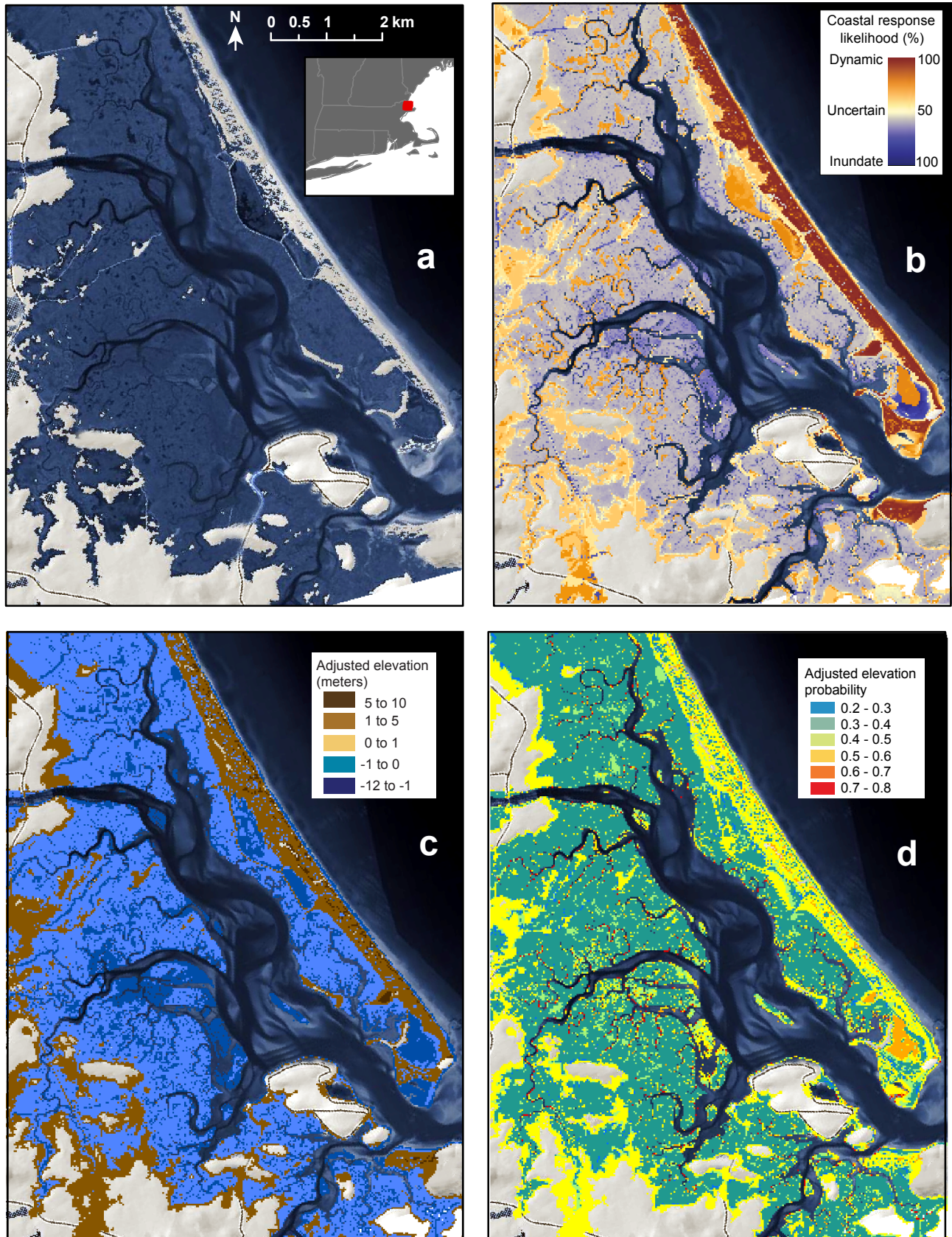


Figure 2. Comparison showing: a) Surging Seas inundation map under 1.5 m of SLR (used with permission: <http://ss2.climatecentral.org/#13/42.7573/-70.8059?show=satellite&level=4&pois=show>); b) predicted coastal response likelihoods for 2080s sea level scenario (comparable projected SL to a); c) most-probable 2080s adjusted elevation (AE, or inundation levels); and d) probabilities of the AE values in (c).

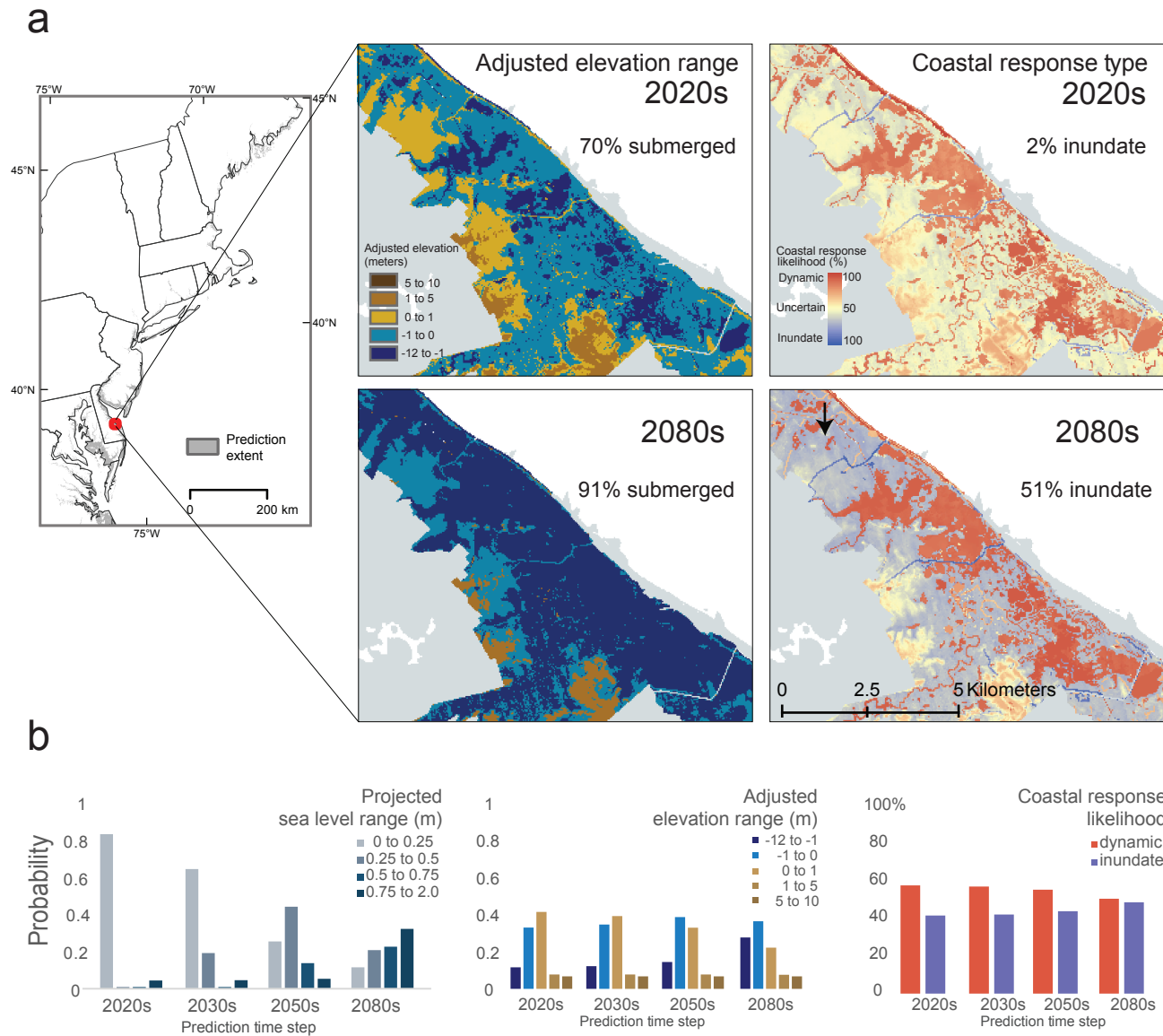


Figure 3. Regional map (a) showing the spatial extent of predictions (gray shading) and examples of adjusted elevation (AE) and coastal response (CR) predictions for the 2020s and 2080s at Prime Hook National Wildlife Refuge in Delaware. The modeled probability distributions (b) for sea level (SL), AE, and CR are shown for each time step at a single cell location (black arrow in lower right panel of (a) indicates location).

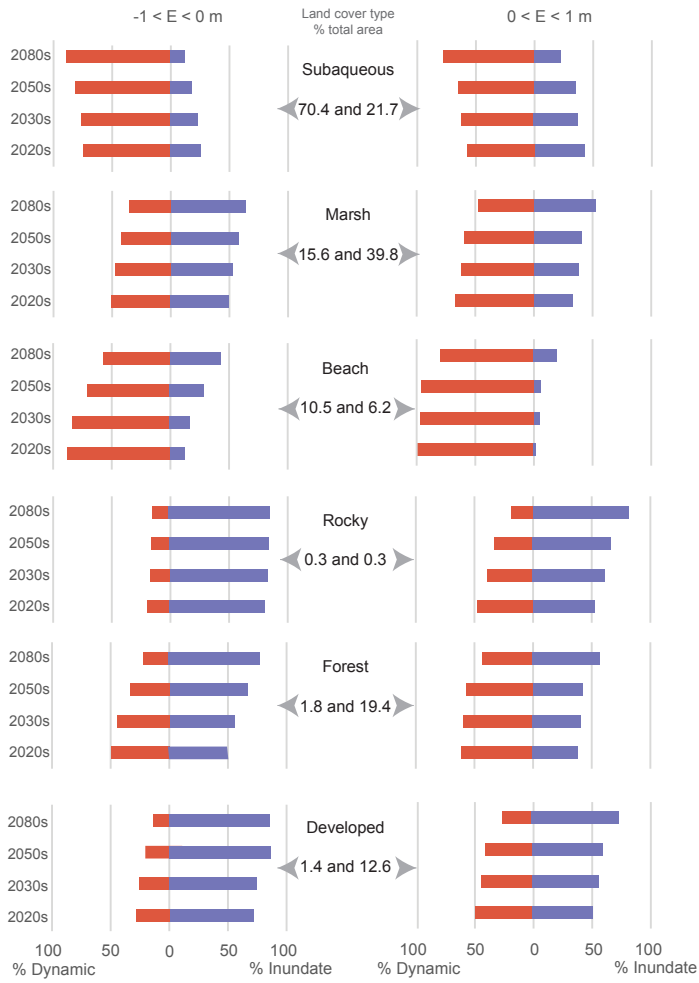


Figure 4. Plots showing shifting coastal response (CR) likelihoods for each land cover type through time conditioned on moderate initial (present day) elevations (E). Central column shows the total percent of the prediction area comprised by each land-cover type by each E range. Red shows probability of dynamic response and blue shows probability of inundation.